HIGH-EFFICIENCY DIODE-PUMPED RUBIDIUM LASER: EXPERIMENTAL RESULTS (Preprint)

Ty A. Perschbacher, David A. Hostutler and Thomas M. Shay

29 January 2007

Conference Paper

AIR FORCE RESEARCH LABORATORY
Directed Energy Directorate
3550 Aberdeen Ave SE
AIR FORCE MATERIEL COMMAND
KIRTLAND AIR FORCE BASE, NM 87117-5776

REPORT DOCUMENTATION PAGE

Form Approved
OMB No. 0704-0188

1. REPORT DATE *(DD-MM-YYYY)*	2. REPORT TYPE	3. DATES COVERED *(From - To)*
29-01-2007	Conference Paper	01-10-2004 – 29-01-2007

4. TITLE AND SUBTITLE

High-efficiency diode-pumped rubidium laser: experimental results (Preprint)

5a. CONTRACT NUMBER
In-House DF297832

5b. GRANT NUMBER

5c. PROGRAM ELEMENT NUMBER

6. AUTHOR(S)
Ty Perschbacher, David A. Hostutler, and T. M. Shay

5d. PROJECT NUMBER

5e. TASK NUMBER

5f. WORK UNIT NUMBER

7. PERFORMING ORGANIZATION NAME(S) AND ADDRESS(ES)

AFRL/DELC
3550 Aberdeen Ave SE
Air Force Materiel Command
Kirtland AFB, NM 87117-5776

8. PERFORMING ORGANIZATION REPORT NUMBER

9. SPONSORING / MONITORING AGENCY NAME(S) AND ADDRESS(ES)

Air Force Research Laboratory
3550 Aberdeen Ave SE
Kirtland AFB, NM 87117-5776

10. SPONSOR/MONITOR'S ACRONYM(S)
AFRL/DELC

11. SPONSOR/MONITOR'S REPORT NUMBER(S)
AFRL-DE-PS-TP-2007-1005

12. DISTRIBUTION / AVAILABILITY STATEMENT
Approved for Public Release; Distribution is Unlimited

13. SUPPLEMENTARY NOTES Presented at XVI International Symposium on Gas Flow and Chemical Lasers & High Power Laser Conference, Sept 5, 2006, Gmuden, Austria.   GOVERNMENT PURPOSE RIGHTS

14. ABSTRACT
A diode-pumped rubidium laser with an optical slope efficiency of 69% has been constructed. This study utilized a narrow-line diode laser pump source for the experiments. The trade space study included optimization of various parameters such as lasing cell composition, temperature, and output coupler reflectivities. The results of the experimental study are given.

15. SUBJECT TERMS
Diode-pumped, rubidium laser, DPAL

16. SECURITY CLASSIFICATION OF:			17. LIMITATION OF ABSTRACT	18. NUMBER OF PAGES	19a. NAME OF RESPONSIBLE PERSON David Hostutler
a. REPORT Unclassified	**b. ABSTRACT** Unclassified	**c. THIS PAGE** Unclassified	SAR	8	**19b. TELEPHONE NUMBER** *(include area code)*

Standard Form 298 (Rev. 8-98)
Prescribed by ANSI Std. 239.18

High-efficiency diode-pumped rubidium laser: experimental results

Ty A. Perschbacher, David A. Hostutler, T. M. Shay
Air Force Research Laboratory, Directed Energy Directorate
Kirtland Air Force Base, New Mexico, USA 87117

ABSTRACT

A diode-pumped rubidium laser with an optical slope efficiency of 69% has been constructed. This study utilized a narrow-line diode laser pump source for the experiments. The trade space study included optimization of various parameters such as lasing cell composition, temperature, and output coupler reflectivities. The results of the experimental study are given.

Keywords: Diode-pumped, rubidium laser, DPAL

1. INTRODUCTION

Diode-Pumped Alkali Lasers (DPAL) are rapidly gaining attention as highly-efficient lasers as well as brightness converters. These systems partly owe their high efficiencies to the very small quantum defects between the upper level spin-orbit states (2% for Rb and 5% for Cs). Diode pumping can provide an efficient, yet compact method for power insertion, while low pressure gaseous gain media allow optimal beam quality by minimizing thermal gradients and beam distortions. Additionally, the output wavelengths for the species of interest (795 nm for Rb and 895 nm for Cs) exhibit excellent atmospheric propagation with minimal attenuation due to molecular absorption. Furthermore, these wavelengths demonstrate excellent materials coupling characteristics. With these properties, a wide variety of applications are possible from materials processing to the medical field where alkali species are under investigation for their role in the polarization of ^{129}Xe in magnetic resonance imaging (MRI) systems [1].

Since their inception in 2003 by Krupke, et al., several groups have conducted various experiments in this field with very promising results [2,3]. For the initial experiments, a Ti:Sapphire surrogate was used to pump the pressure broadened absorption transition of the alkali species. Optical slope efficiencies of 54% for Rb and 59% for Cs with respect to absorbed pump power were reported [2,4]. In 2006, Ehrenreich et al. presented a narrow-banded (~ 1 MHz) diode pumped Cs laser with a slope efficiency exceeding 80% [5]. Also in 2006, Page et al. reported on the first DPAL system pumped with a multimode diode array [6]. Although optical efficiencies were lower, the radiance of the output laser was still 2000 times greater than the pump. Finally, Wang et al. produced a Cs laser using a Volume Bragg Grating coupled laser diode array [7].

As outlined in Figure 1., the alkali vapor lasers are pumped on the D_2 transition from the $^2S_{1/2}$ to the $^2P_{3/2}$ state, ideally using diode laser excitation. The relaxation from the pump level to the upper laser level in the alkali vapor lasers is achieved by means of spin-orbit coupling between the $^2P_{3/2}$ and $^2P_{1/2}$ states. Due to the short lifetimes of the $^2P_{3/2}$ states (~26 ns for Rb and ~30 ns for Cs), which decay back to the ground $^2S_{1/2}$ state, this process must be accelerated using some species to increase the rate of spin-orbit relaxation. In the case of Cs in the presence of 500 torr of helium and 70 torr of ethane at 110 ºC, ethane has proven the most effective species for promoting this transition, accelerating the relaxation to 33 times faster than the radiative decay rate out of the $^2P_{3/2}$ state [4,8]. Lasing is then achievable on the D_1 transition between the $^2P_{1/2}$ and $^2S_{1/2}$ states. Currently, mismatch between the natural absorption linewidths of the alkali vapors (~0.4 GHz) and the available spectral bandwidths of commercial-off-the-shelf diode lasers (>1000 GHz) limits the optical and overall efficiency of these laser systems. Accordingly, efforts to better match the linewidths of the alkali absorption transition and diode pump are necessary to ensure peak performance. To date, either helium is used as a means to homogenously broaden the alkali vapor absorption spectrum or external cavity, narrow-banding elements are used to narrow the diode laser emission spectrum.
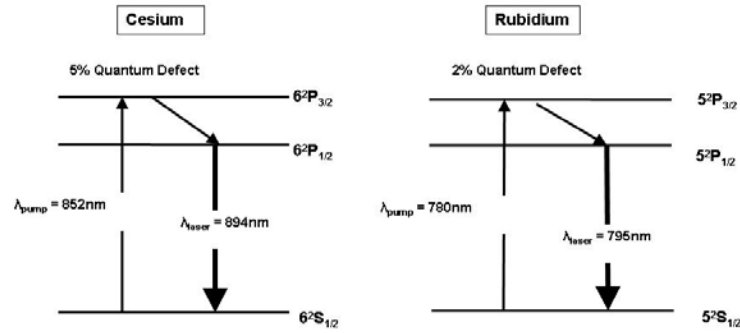
Fig. 1. Energy level diagrams of Cs and Rb showing transitions of pumping and lasing

As mentioned earlier, experiments have been conducted using Cs as the gain medium with both narrow-line pumping and He pressure broadening. However all previous Rb experiments have been conducted using He broadening with broad pump sources. This paper gives the results of a study conducted using a narrow-line pump source with a low pressure gain cell.

2. EXPERIMENTAL SET-UP

For these experiments, the optical setup outlined in Figure 2 was used. In short, the output from a narrow-banded diode laser was coupled into a heated Rb cell containing some ratio of helium and ethane by means of a focusing lens and polarization beam splitter. The diode laser (Sacher Laser, Tiger Series) utilized a Littrow-style external cavity configuration to produce ~ 1.2 watts of monochromatic radiation with a linewidth of ~ 1 MHz at 780 nm. A half-waveplate was used to rotate the polarization of the beam to the s-polarized configuration. A lens focused the beam to achieve the desired pump power density within the heated cell. The pump source was introduced into the cavity using a polarization beam splitting cube (Lattice Electrooptics) allowing p-polarized 795 nm light to pass while redirecting the s-polarized light into the system. The Rb sample cells (Triad Technologies) with varying compositions of helium and ethane, and AR-coated windows were placed in an aluminum oven and heated to optimal temperatures based on the cell compositions. Each quartz cell was 2.5cm in diameter and length. After the first pass, the remaining pump power was redirected back into the cavity for the second pass using a flat, high reflector (99.5% Lattice Electrooptics). The curved output coupler (20 cm rc Lattice Electrooptics.) was located 12.5cm from the high reflector.
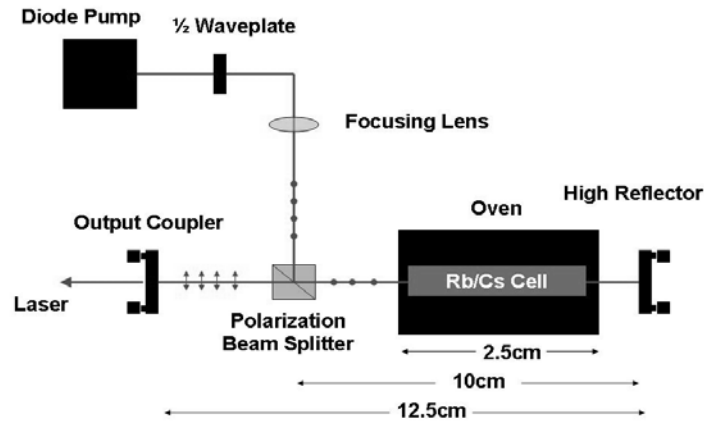

Figure 2. Schematic of Experimental Setup used for Rb laser demonstration

For optimal laser performance, the pump beam was focused to a spot size diameter of ~130 μm at the cell entrance resulting in a power pump density of ~10 kW/cm^2. Since the beam waist was focused to a point in front of the cell, the beam expanded to 166 μm at the cell exit resulting in a pump power density of ~6 kW/cm^2. A variety of cell compositions varying ethane and helium pressures, as well as output coupler reflectivities (10, 20, 30, 50, 70, and 90%) were investigated. The different cell configurations were employed to examine trends associated with varying amounts of buffer and spin-orbit mixing constituents. Table 1 lists the test cell compositions examined in this study.

For each cell and output coupler configuration, gross alignment was used to initiate lasing and the output power was measured using a power meter (Ophir Laser Star with Ophir head). After lasing was established, output power was optimized by initially adjusting the cell temperature. When optimal cell temperature was determined and set, laser output power was again optimized by fine tuning the diode laser's output wavelength using a piezoelectric actuator. By adjusting the diffraction grating incidence angle using the piezoelectric actuator, the output wavelength was continuously tuned through a range of wavelengths due to the change in wavelength reflected by the blazed grating that was subsequently re-injected into the diode.

Table 1. Pressure (in torr)of ethane and helium in various sample cells. Ethane and helium pressures are indicated on the vertical and horizontal axes, respectively. Temperatures optimizing laser output power are given in º Celsius. Only cells with accompanying temperature data were tested.

ethane/He	0	50	100	200	400
400	109	122			
300	107				
200		122			
150					
100	102	122		122	
50			122		134

Power curve measurements documenting output power versus input power were recorded. No less than three sets of measurements were recorded for each cell and output coupler. Slope and actual efficiencies were calculated from each data set. The slope efficiencies for each cell and output coupler were averaged and presented as functions of output coupler reflectivity, ethane pressure, and helium pressure.

3. EXPERIMENTAL RESULTS

Due to the narrow spectrum of the pump radiation (~1 MHz) falling completely within one component of the Rb absorption band (> 500 MHz), 95% of the pump radiation was absorbed on the first pass. The resonator was configured with the high reflector re-depositing the remainder of the pump radiation back into the cell for further absorption resulting in ~99.8% absorption of the input radiation. The one-way cavity loss associated with transmission through the polarization beam splitting cube, oven, and cell of 11% was measured using the diode laser as a probe through a cold cell. The loss measurement was made on the 780 nm pump line versus the 795 nm stimulated emission line due to the diode laser's inability to tune to the necessary frequency.

The maximum laser power obtained was 490 mW. This corresponded to the 400/0 torr ethane/helium cell, a 30% reflective output coupler, 1260 mW of pump power and a cell temperature of 109 ºC. The highest slope efficiency obtained was 69% using the 400/50 ethane/helium cell and a 20% reflective output coupler. The optimized cell temperature for the 400/50 ethane/helium cell was 122 ºC. The optical-optical efficiency for this set-up was 31.5%. with a rather large threshold power of ~677 mW. Figure 3 illustrates experimental power curves for the 400/50 cell with varying output coupler reflectivities.

Power measurements were obtained by measuring the input power upstream of the polarization beam splitting cube and Rb laser output power downstream of the output coupler.
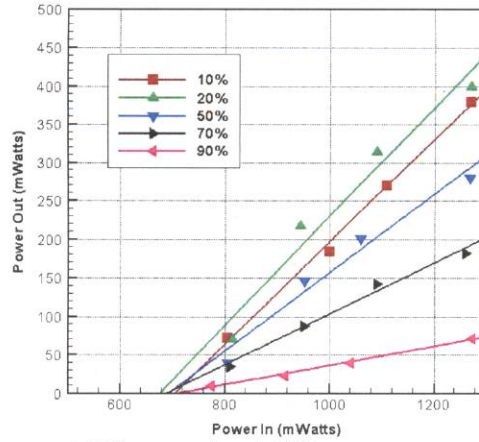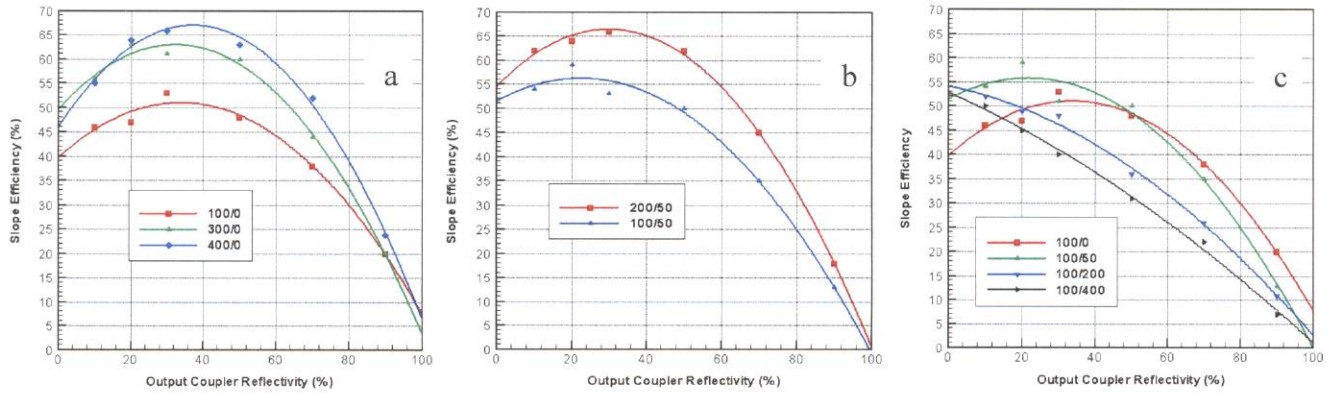

Figure 3. Rb laser output power at 795 nm vs. input 780 nm pump power for various output couplers.

Figures 4(a-c). Averaged optical-optical slope efficiencies for diode pumped Rb laser versus output coupler reflectivity with (a) variation of ethane with no helium; (b) variation of ethane with 50 torr of helium; and (c) variation of helium with 100 torr of ethane.

4. ANALYSIS AND DISCUSSION

Once measured, calculated, and averaged, the slope efficiency data was plotted as functions of output coupler reflectivity, ethane pressure, and helium pressure for trend analysis. The resulting data plots can be observed in Figures 4(a-c). Upon initial examination of the trend curves in Figure 4a, it appears increased amounts of ethane tend to promote improved performance in the laser. As shown in the figure, increasing the ethane pressure in the absence of helium improves performance substantially. This is most likely due to more rapid spin-orbit quenching with higher amounts of ethane. However, the effect of the ethane is two-fold as a result of the subsequent pressure broadening of the Rb absorption transition. This effect tends to lower the line center absorption transition, reducing the effectiveness of the pump. In the absence of helium, the effect of the ethane is still a positive one with pressures as high as 400 torr, but a rollover point would likely be observed at higher ethane pressures as the rate of spin-orbit quenching is optimized and additional ethane merely acts to lower peak absorption.

Continuing on with Figure 4b, the ethane pressure was reduced and helium in the amount 50 torr was introduced into the cell. Similar to Figure 4a an increase in ethane (i.e. 200 torr vs. 100 torr) appears to increase performance. It should also be noted at this point that the cells containing helium optimized at temperatures of ~120ºC as opposed to the cells containing no helium which optimize at ~110 ºC. This increase in temperature leads directly to a higher number density of gas phase Rb atoms. Taking into consideration the fact that helium will primarily act to broaden and lower the peak of the Rb absorption curve, it can be concluded there is a optimum balance between lowering peak gain/absorption due to pressure broadening and increasing number density available for lasing.

An apparent dichotomy between the ethane and helium appears to occur. While the reduction in ethane from 400 torr to 200 torr would have been responsible for lowering laser performance, the added helium appears to actually improve overall performance to that of the 400/0 ethane/helium torr cells despite the reduced amount of ethane by a factor of 2. This effect can be best rationalized by considering the higher temperature requirements associated with adding helium into the cell. While the reduction in ethane should act to reduce the spin-orbit coupling rates, it should also result in a nominal increase in peak absorption due to the lower pressure broadening. In turn, the helium addition should result in a significant increase in broadening along with the associated decrease in peak absorption. However, as seen in Table 1, even minor additions of helium result in the requirement for higher optimal cell temperatures, and hence, higher Rb vapor densities. As such, while the helium acts to effectively lower laser performance due to the broadening effect, the requirement for higher temperatures counteracts the performance lowering effects by proving more Rb atoms to be excited. Laser performance is, of course, affected by the competition between these two effects. An optimal configuration/cell composition should exist based on the optimal amounts of ethane and helium.

Finally, in Figure 4c, it is clear that helium improves performance to a point, but eventually degrades performance as higher pressures are introduced. This is likely due to the broadening and subsequent lowering of the Rb absorption curves. One note should be made as to the importance of helium in scaling these lasers to higher powers. While in the case of very narrow-band, low-power, diode sources, helium primarily acts to lower performance. However; helium will eventually be a crucial ingredient due to the current lack of availability of high-power, narrow-band diode laser sources and increased thermal effects in the cavity associated with higher intensities. The positive effects of helium will assist in matching the absorption and pump linewidths as well as reducing negative thermal effects.

The threshold pump power obtained for all cells was typically very high ranging from greater than 400 to less than 750 milliwatts. While the measured one-way cavity losses suggests relatively low cavity losses at 11%, the relatively high threshold powers imply some other form of loss is at work. One potential source revolves around collisional re-excitation from the upper laser level $^2P_{1/2}$ to the pump level $^2P_{3/2}$ via collisions with ethane due to the very small quantum defect between the spin-orbit states. A more in-depth model describing this process will be investigated in the future.

If the threshold power can be reduced by lowering cavity losses, dichroic optics designed to pass 780nm radiation while reflecting 795nm radiation could be utilized. Eliminating the 3 surfaces introduced in the resonator by the beam splitting prism should significantly reduce such optical cavity losses.

While the spectral bandwidth of the pump source for this study was many times narrower than the effective pressure-broadened cells consisting of Rb, ethane, and helium at elevated temperatures, the requirements for such narrow bandwidths for future work are not as strict. In fact, the pump source requirements for effective spectral bandwidth matching can be greatly reduced by considering the pressure broadening associated with the constituents required for effective laser operation.

5. CONCLUSIONS

This device represents a diode-pumped Rb laser with the highest optical slope efficiency reported to date. The high (>65%) slope, efficiencies obtained by this device can be attributed to the extremely narrow 1 MHz linewidth of the pump laser source and the subsequent optimal pump/absorption overlap between the pump source and Rb/ethane/helium absorption spectra. Parameters such as lasing cell mixtures and temperatures were explored to determine their effects on overall performance. Finally an initial paper investigation was explored on determining pump linewidth requirements with the various Rb/Helium/Eth and mixtures that were studied.

6. ACKNOWLEDGEMENTS

7. REFERENCES

1. D. Levron, D.K. Walter, S. Appelt, R.J. Fitzgerald, D. Kahn, S.E. Korbly, K.L. Sauer, W. Happer, T.L. Earles, L.J. Mawst, D. Boetz, M. Harvey, L. DiMarco, J.C. Connolly, H.E. Moller, X.J. Chen, G.P. Cofer, and G.A. Johson, "Magnetic Resonance Imaging of Hyperpolarized 129-Xe Produced by Spin Exchange with diode-laser pumped Cs," Applied Physics Letters, vol 73, No. 18, p. 2666, (1998).
2. W.F. Krupke, R.J. Beach, V.K. Kanz, and S.A. Payne, "Resonance Transition 795-nm Rubidium Laser," Optics Letters, Vol. 28, No. 23, p. 2336, (2003) *and references within*.
3. W.F Krupke, R.J. Beach, V.K. Kanz, S.A. Payne, J.T. Early, "New Class of CW High-Power Diode Pumped Alkali Lasers (DPALs)," SPIE High-Power Laser Ablation V Proceedings, Vol. 5448, p. 7, (2004) *and references within*.
4. R.J. Beach, W.F. Krupke, V.K. Kanz, S.A. Payne, M.A. Dubinskii, and L.D. Merkle, "End-Pumped continuous-wave alkali vapor lasers: experiment, model, and power scaling," Journal of the Optical Society of America B, Vol. 21, No. 12, (2004).
5. T. Ehrenreich, B. Zhdanov, R.J. Knize, "Highly Efficient Cesium Vapor Laser," SPIE Laser Bean Control and Applications Proceedings, Vol. 6101, (2006).
6. R.H. Page, R.J. Beach, V.K. Kanz, and W.F. Krupke, "Multimode-Diode Pumped Gas (Alkali-Vapor) Laser," Optics Letters, Vol. 31, No. 3, p. 353, (2006).
7. Y. Wang, T. Kasamatsu, Y.Zheng, H. Miyajima, H. Fukuoka, S. Matsuoka, M. Niigaki, H. Kubomura, and H. Kan, "Cesium Vapor Laser Pumped by a Volume-Bragg-Grating Coupled Quasi-Continuous-Wave Laser Diode Array," Applied Physics Letters, **88,** 141112, (2006).
8. E. Walentynowicz, R.A. Phaneuf, and L. Krause, "Inelastic collisions between excited alkali atoms and molecules. X-temperature dependence of cross sections for $^2P_{3/2} - ^2P_{1/2}$ mixing in cesium, induced in collisions with deuterated hydrogens, ethanes, and propanes." Can. Journal of Physics, **52,** 589-591, (1974).